

MODELING OF THE DYNAMIC RESPONSE OF A PELTON TURBINE HYDROELECTRIC PLANT

P. Pennacchi, S. Chatterton, A. Vania

Politecnico di Milano, Department of Mechanical Engineering
 Via La Masa, 1, I-20156, Milano, Italy

ABSTRACT

The paper presents a detailed numerical model of the dynamics of a Pelton turbine installed in a hydroelectric plant. The model considers in detail the Pelton turbine with all the electromechanical subsystems, such as the main speed governor, the controller and the servoactuator of the turbine nozzle, and the electric generator. In particular it reproduces the effects of pipe elasticity in the penstock, the water inertia and the water compressibility on the turbine behaviour. The dynamics of the surge tank on low frequency pressure waves is also modeled together with the main governor speed loop and the position controllers of the nozzle needle actuators and of the hydraulic electrovalve. Model validation has been made by means of experimental data acquired during some starting tests after a partial revamping of a hydroelectric unit, which involved also the control system of the hydraulic actuators but not the nozzles. The model is used in order to identify the cause of the oscillations of the electric power mainly ascribed to the backlash of the nozzle needle system.

NOMENCLATURE

| | |
|---------------------------|--|
| $\Delta\bar{\omega}$ | Deviation of rotational speed in p.u. |
| $\Delta\bar{G}$ | Deviation of gate opening in p.u. |
| $\Delta\bar{H}_i$ | Deviation of turbine hydraulic head in p.u. |
| $\Delta\bar{p}_i$ | Deviation of normalized pressure at gate |
| $\Delta\bar{P}_m$ | Deviation of mechanical power in p.u. |
| $\Delta\bar{U}_i$ | Deviation of water velocity in p.u. |
| ϕ_p | Friction energy term of the penstock |
| ρ | Volumetric mass of water |
| τ_p | Time constant of the servovalve |
| ω_0 | Rotational speed in operating condition |
| A_p | Penstock area |
| b_p, b_i, T_x, T_d, T_3 | Gains and time constants of the speed controller |
| C_i | Proportional gain of the servovalve controller |
| C_x | Flow gain of the servovalve |
| c_p | Wave velocity in the penstock |
| D | Damping factor |
| D_c | Tunnel diameter |

| | |
|--------------------------------|---|
| D_p | Penstock diameter |
| \bar{e}_ω | Rotational speed error in p.u. |
| E | Young's modulus of elasticity of pipe material |
| f | Thickness of pipe wall |
| g | Gravitational acceleration |
| G_n, \bar{G}_n | Gate opening reference signal and p.u. form |
| G | Equivalent gate opening |
| G_k | Position of the k -th needle |
| H_0 | Hydraulic head in operating condition |
| H | Hydraulic head at gate |
| I_0 | Current command input of the servovalve |
| J | Generator inertia |
| k_1 | Gain constant of the servovalve |
| k_2, k_3, k_8, a_i | Constants and i -th coefficient of the hydraulic axial thrust |
| k_4, k_5 | Constants of the elastic force of Bellville washers |
| k_6 | Constant of the outlet oil flow |
| k_7 | Bellville washer preload |
| k_b | Hydraulic cylinder net area constant |
| k_f | Friction coefficient of the penstock |
| k_p, k_i | Gains of the PI speed controller |
| K | Bulk modulus of water compression |
| K_i | Inertia constant |
| K_u, K_p | Velocity and power constants |
| L_c | Tunnel length |
| L_p | Penstock length |
| N_{el}, N_{th} | Elastic force and hydraulic axial thrust |
| $P_m, (P_{m0})$ | Turbine mechanical power (in operating condition) |
| $q_{oil}, q_{open}, q_{close}$ | Oil flows in the nozzle hydraulic cylinder |
| Q_0 | Turbine water flow in operating condition |
| \bar{T}_e | Electrical load torque in p.u. |
| T_{ep} | Elastic time of the penstock |
| \bar{T}_m | Mechanical torque of the turbine in p.u. |
| T_s | Time constant of the surge tank |
| T_{wc} | Starting time of the tunnel |
| U | Water velocity |
| x | Pilot valve spool position |
| Z_p | Penstock normalized hydraulic surge impedance |
| Z_{p0} | Hydraulic surge impedance of the penstock |

INTRODUCTION

The accurate dynamic model of turbine units in hydroelectric plants assumes great importance in case of renewal of turbine components, such as the control and the actuator systems, or in case of periodic and required inspections of the emergency systems. In this sense, a model of the entire system prevents dangerous conditions during the control system tuning and provides a reference response for inspections. This kind of model could be also used during design phases, for penstock dimensioning, for the overspeed estimation or for the analysis of new control strategies of the speed governor.

The first studies about power system of hydro turbines date back to the early 70s, when a task force on overall plant response was established in order to consider the effects of power plants on power grid stability and to provide recommendations regarding problems not already investigated. The outcome of this effort has been a first simple model consisting of transfer functions of the speed governing systems and hydro turbines systems [1].

These early models were inadequate to study large variations of power output and frequency. For instance they were not reliable in the very low frequency range, as they did not account for water mass oscillations between the surge tank and the reservoir, and at high frequency [2], as they did not reproduce water hammer effects.

To solve these limitations, some improvements of both turbine and speed control models were made by the Working Group on Prime Mover and Energy Supply Models for System Dynamic Performances Studies [3].

In the paper, the authors propose a detailed and complete numerical model of the dynamic behaviour of a Pelton turbine belonging to a hydroelectric plant. The model considers in detail the Pelton turbine, all the electromechanical subsystems, such as the main speed governor, the controller and the servoactuator of the nozzle needle, and the electric generator. In particular it reproduces the effects of pipe elasticity in the penstock, the water inertia and the water compressibility on the turbine behaviour. The dynamic of the surge tank and the reservoir on low frequency pressure waves are also modeled together with the main governor speed loop and the position controllers of the distributor actuator and of the hydraulic electrovalve. The proposed model has been successfully validated by means of experimental data of a 67.5 MW – 540 m hydraulic head Pelton turbine of a hydroelectric plant, acquired during some starting tests after revamping, which involved also the control system of the distributor. In particular the model has been used in order to identify the cause of the oscillations of the electric active power, mainly ascribed to the backlash of the nozzle needle system, which was not revamped.

PLANT DESCRIPTION

The Pelton turbine unit here considered belongs to a complex hydroelectric basin, in southern Italy, consisting of three hydroelectric plants, placed in series.

The first hydroelectric plant, analysed by the authors in [4], is constituted of two 75 MW Francis turbines with a hydraulic head of about 470 m.

The discharged water of the first plant supplies a second reservoir used by the second plant. The discharge of the second plant supplies a third water reservoir used by the last plant constituted again of a 50 MW and a 17 MW Francis turbines with a hydraulic head of about 150 m.

The second plant described in the paper is constituted of two 67.5 MW and a 78.5 MW multijet vertical axis Pelton turbines with a hydraulic head of about 540 m, supplied by two steel penstocks from two interconnected surge tanks, each of them connected to the water reservoir by two rocky tunnels [5] as shown in the Figure 1. The main data of the plant are also reported in Table 1.

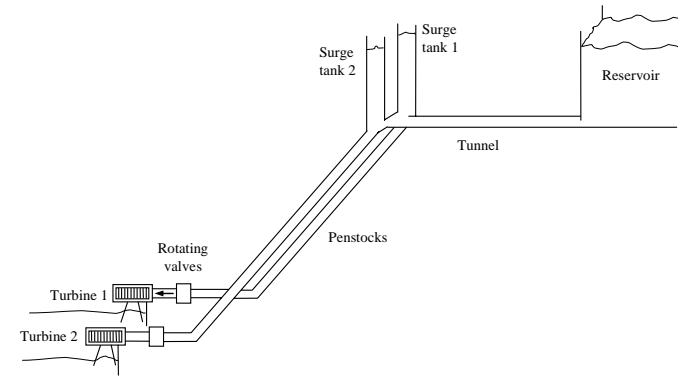


Figure 1. Hydraulic scheme of the first plant.

Considering the scheme of Figure 2, the 6 jet Pelton turbine unit is composed of the runner equipped with 21 buckets (Figure 3), the 6 nozzles and the ball valve (Figure 4). This valve operates only during starting, emergency phases and stopping.

Table 1. Data of the hydroelectric plant.

| | | |
|------------|-----------------------------------|--------------------------------------|
| L_c | Tunnel length | 4000 m |
| D_c | Tunnel diameter | 5.5 m |
| L_p | Penstock length | 1470 m |
| D_p | Penstock diameter | 3.2 m |
| f | Thickness of pipe wall | 0.035 m |
| Q_{0r} | Rated flow | 14.4 m ³ /s |
| H_0 | Hydraulic head | 538-511 m |
| J_{PD^2} | Generator inertia PD ² | 550 10 ³ kgm ² |
| Q_0 | Single turbine rated flow | 14.4-14 m ³ /s |
| P_r | Single turbine electric power | 67.5-62.5 MW |
| ω_0 | Rated speed | 500 rpm |

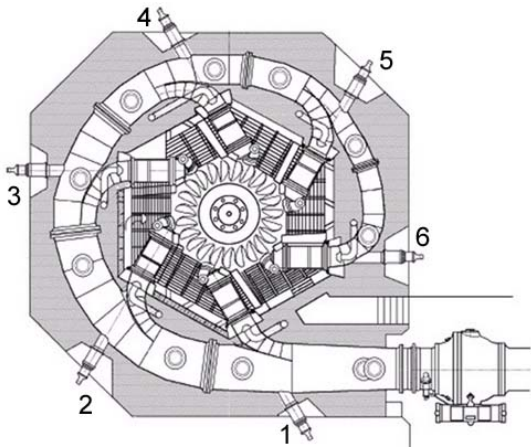


Figure 2. Scheme of the 6 jet Pelton turbine unit.



Figure 3. Pelton runner equipped with 21 buckets.



Figure 4. Ball valve at the end of each penstock.

The generator of each unit, shown in Figure 5, is a 70 MVA - 10 kV - 50 Hz three-phase synchronous machine running at 500 rpm. In the same figure it is possible to identify the upper part of the exciter system of the generator.



Figure 5. 70 MVA - 10 kV generator of the first 67.5 MW - 50 Hz unit running at 500 rpm.

As said before, the experimental tests described in the next section were performed after the renewal of the control system unit of the actuators of the nozzle needles and the deflector plate. However no mechanical maintenance had been performed on the nozzles.

MODEL OF THE SYSTEM

The functional block diagram of the overall system of the hydroelectric plant is shown in Figure 6, where the single turbine unit is considered [6]. It mainly consists of the speed changer, the speed regulator, the needle actuator system, the turbine and the generator.

For the safety of the electric network, the frequency should remain almost constant. This is ensured by keeping constant the speed of the synchronous generator.

The speed changer (external remote control) gives the reference speed signal, depending on the power network requirements, since the frequency depends on the active power balance of the network.

The rotational speed of the turbine is fed back and modified by the speed governor acting on the nozzle needles (gates) by means of hydraulic actuators. The turbine mechanical power is essentially a function of nozzle positions.

In the following sections the details of each submodel are analysed.

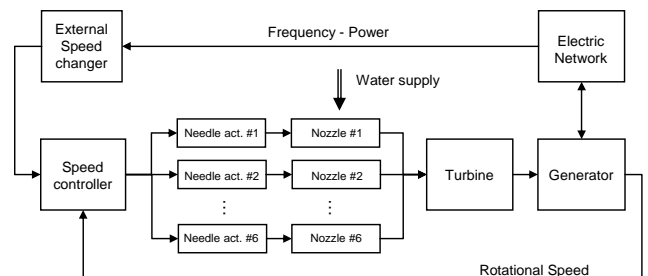


Figure 6. Functional block diagram of the overall system.

Speed controller model

The actual speed regulator implemented in the model consists of two operating modes: the *starting mode* for run-ups from standstill to steady state condition without load, and the *operating mode* for nominal operating condition at rated speed and with an active load. The switching between the two operating modes is done in a bumpless way. The starting mode consists of a simple PI regulator:

$$F_{starting}(s) = \frac{\bar{G}_0}{\bar{e}_\omega} = k_p + \frac{k_i}{s} \quad (1)$$

where \bar{G}_0 is the normalized gate opening reference signal and \bar{e}_ω is the error of the normalized rotational speed. A simple anti-windup compensation, that stops the integration when a threshold is reached, is included in the model.

The speed controller in the operating mode is realized by the following two-pole and two-zero transfer function:

$$F_{operating}(s) = \frac{\bar{G}_0}{\bar{e}_\omega} = \frac{1}{b_p} \frac{\left(\frac{T_x}{b_t} s + 1 \right) (T_d s + 1)}{\left(\frac{T_x}{b_p} s + 1 \right) (T_3 s + 1)} \quad (2)$$

The final control scheme, including the speed compensation, is shown in Figure 7, where two compensation terms are added to the reference signal of the gate opening. The steady state compensation allows to reduce the steady state rotational speed error owing to the droop characteristics, whereas the variable compensation is a feed forward term depending on the electrical load.

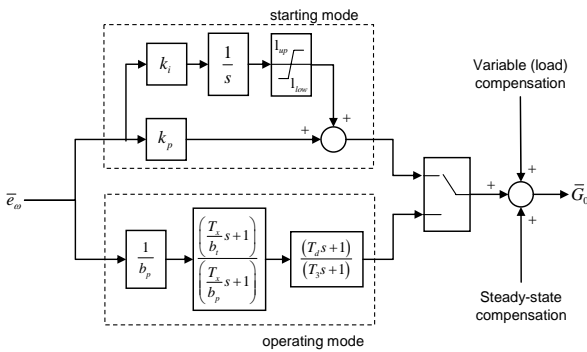


Figure 7. Speed controller block diagram.

Actuator system model of the nozzle needles

The rotational speed of the turbine is controlled by modifying the water flow striking the runner buckets, by means of 6 needles as shown in Figure 8. When the needle is pushed forward, the amount of water striking the runner is reduced and when the needle is pushed back, the amount of water striking the runner increases.

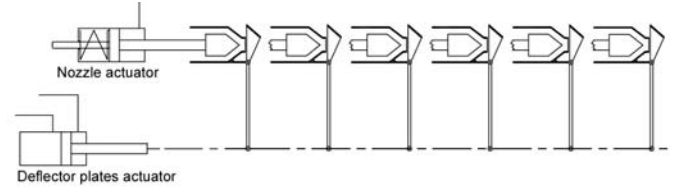


Figure 8. Scheme of the actuator systems of the nozzle needles and the deflector plates.

A small nozzle is installed to stop the runner in a short time, directing the jet of water on the back of the vanes. The nozzles are also equipped with a deflector plate, a safety system that is able to divert the water jet striking the runner buckets, in order to avoid high pressure waves in the penstock owing to an emergency fast needle closure. The deflector plates are moved by a common hydraulic actuator.

The output of the speed regulator block is proportional to the opening reference signal of the nozzle needle.

The opening of each nozzle needle is performed by independent hydraulic actuators, whereas, for safety reasons, the closure is realized by Belleville washers.

The actuators are position controlled, modifying the cylinder oil flow with an electrovalve by means of a simple proportional position controller:

$$I_0(s) = C_I (G_0 - G_k) \quad (3)$$

where G_0 and G_k are the reference and the actual gate opening respectively, C_I is the gain of the controller and I_0 is the current reference signal of the servovalve.

The speed of the cylinder stem depends on the direction of the movement; in particular it is proportional to the inlet (for the opening movement) or the outlet (for the closure movement) oil flow in the cylinder chamber. Thus, the simplest first order transfer function that relates the k -th needle position G_k and the oil flow q_{oil} could be written as:

$$F_c(s) = \frac{G_k(s)}{q_{oil}(s)} = k_b \frac{1}{s} \quad (4)$$

where k_b is a suitable constant representing the cylinder net area and the assumed linear relationship between the needle position and the gate opening.

For the opening movement, the inlet oil flow could be assumed proportional to the position x of the electrovalve spool:

$$q_{open} = C_x x \quad (5)$$

where C_x is the flow gain of the electrovalve.

The closure movement is given by the elastic force exerted by Bellville washers acting on the cylinder stem. The following experimental formula describes the involved elastic force:

$$N_{el} = k_4 \ln \left(1 + \frac{G_k}{k_5} \right) + k_7 \quad (6)$$

where k_7 represent the washer preload.

The hydraulic axial thrust acting on the needle, and therefore also on the cylinder stem when the needle is opened, could be approximated by a polynomial expression [10]:

$$N_{th} = k_8 \sum_{i=0}^6 a_i \left(\frac{G_k}{k_3} \right)^i - k_2 \quad (7)$$

Being the pressure of the oil in the cylinder chamber proportional to the outlet oil flow, neglecting inertial forces, the oil flow for the closure movement is:

$$q_{close} = \frac{C_x}{k_6} (N_{el} - N_{th}) x \quad (8)$$

The servovalve spool is position controlled. The global behaviour of the servovalve, including the spool position controller, could be described by a first order transfer function that relates the spool position x to the current input I_0 :

$$F_{I-x}(s) = \frac{I_0(s)}{x(s)} = \frac{k_1}{\tau_p s + 1} \quad (9)$$

where τ_p is the time constant of the servovalve and k_1 a suitable gain. The sign of x also represents the direction of the nozzle needle movement.

The block diagram of the position control loop of each needle, including the servovalve and the actuator transfer functions, is shown in Figure 9. The figure also reports the nonlinearities owing to the limits of the servovalve spool position and to the limits of the speed and position of the needle.

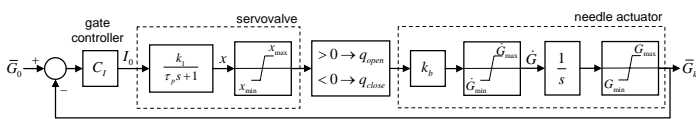


Figure 9. Block diagram of the needle position control loop.

Turbine model

The dynamic behaviour of a hydraulic turbine operating at full load is widely described by a transfer function that relates the deviation of the output mechanical power to the deviation of gate opening [7,8].

The turbine-gate system is modelled as an orifice valve, where the velocity U of the water at gate is given by:

$$U = K_u G \sqrt{H} \quad (10)$$

where G is the equivalent gate opening obtained by the mean

value of the 6 needle G_k openings. The turbine mechanical power is proportional to the product of pressure and flow:

$$P_m = K_p H U \quad (11)$$

where K_u and K_p are constants and H is the hydraulic head at gate.

By linearizing and considering both small displacements around the operating point and per unit (p.u.) expressions, it follows:

$$\frac{\Delta \bar{P}_m(s)}{\Delta \bar{G}(s)} = \frac{1 + \frac{1}{F(s)}}{1 - \frac{1}{2} \frac{1}{F(s)}} \quad (12)$$

where $\Delta \bar{P}_m = \Delta P_m / P_{m,0}$ is the p.u. small deviation of the mechanical power (corresponding to the p.u. mechanical torque), $\Delta \bar{G}$ is the p.u. small deviation of the gate opening and $F(s) = \Delta \bar{U}_t(s) / \Delta \bar{H}_t(s)$ is the transfer function that relates the normalized water flow deviation (corresponding to the p.u. water speed) to the normalized hydraulic head deviation at gate.

The effects of the travelling waves owing to the elasticity of the penstock steel and to the water compressibility have been considered again by means of a transfer function approach. This approach allows only the evaluation of the same quantities at the turbine level [2].

The overall and detailed transfer function to be used in eq. (12) is given by [7]:

$$F(s) = \frac{\Delta \bar{U}_t}{\Delta \bar{H}_t} = - \frac{1 + \frac{F_1(s)}{Z_p} \tanh(T_{ep}s)}{\phi_p + F_1(s) + Z_p \tanh(T_{ep}s)} \quad (13)$$

- $F_1(s)$ is the transfer function that describes the tunnel and the surge tank interaction [7]:

$$F_1(s) = - \frac{\Delta \bar{H}_t}{\Delta \bar{U}_p} = \frac{\phi_c + s T_{wc}}{1 + s T_s \phi_c + s^2 T_{wc} T_s} \quad (14)$$

- $T_{ep} = L_p / c_p$ is the elastic time of the penstock of length L_p ;
- $c_p = \sqrt{g / \alpha_p}$ is the wave velocity in the penstock;
- α_p considers the water compressibility and the pipe elasticity:

$$\alpha_p = \rho g \left(\frac{1}{K} + \frac{D_p}{E f} \right) \quad (15)$$

- Z_p is the normalized value of the hydraulic surge impedance of the penstock given by:

$$Z_p = Z_{p0} \left(\frac{Q_0}{H_0} \right) \quad (16)$$

- $Z_{p0} = c_p / A_p g$ is the hydraulic surge impedance of the penstock;
- ϕ_p represents the friction energy term of the penstock:

$$\phi_p = 2k_f |U_0| \quad (17)$$

The term $\tanh(T_{ep}s)$ in eq. (13) could be written as [2][7]:

$$\tanh(T_{ep}s) = \frac{1 - e^{-2T_{ep}s}}{1 + e^{-2T_{ep}s}} = \frac{sT_e \prod_{n=1}^{\infty} \left[1 + \left(\frac{sT_{ep}}{n\pi} \right)^2 \right]}{\prod_{n=1}^{\infty} \left[1 + \left(\frac{2sT_{ep}}{(2n-1)\pi} \right)^2 \right]} \quad (18)$$

The normalized pressure deviation at gate could be easily evaluated by:

$$\Delta \bar{p}_t = \rho g \Delta \bar{H}_t \quad (19)$$

where the normalized hydraulic head deviation at gate $\Delta \bar{H}_t$ depends on the gate opening and could be evaluated by the following transfer function:

$$F_p(s) = \frac{\Delta \bar{H}_t}{\Delta \bar{G}} = \frac{1}{F(s) - \frac{1}{2}} \quad (20)$$

Load model

The simple torque equilibrium equation at the turbine shaft allows the insertion of both the electrical load torque \bar{T}_e (p.u.) and the inertia of the rotor in the model:

$$\Delta \bar{\omega} = \frac{1}{T_a s + D} (\bar{T}_m - \bar{T}_e) \quad (21)$$

where \bar{T}_m is the p.u. mechanical torque given by the turbine, D the damping factor, $\Delta \bar{\omega}$ the p.u. rotational speed deviation and T_a the mechanical starting time. The mechanical starting time is obtained by the inertia constant $K_i = T_a / 2$ that it is defined by the ratio of the kinetic energy of the rotor at rated speed ω_0 and the rated electric power of the generator $(VA)_0$:

$$K_i = \frac{1}{2} \frac{J \omega_0^2}{(VA)_0} \quad (22)$$

Regarding the electrical load, all electrical devices such as the generator, the transformers and the power network have not been modelled in detail [9]. The experimental electrical load T_e has been used as input in the model simulations.

EXPERIMENTAL TESTS

Experimental data are acquired during some inspection tests of the restoring procedures of the plant control system. The tests are subsequent to a revamping that involved the control system of the hydraulic cylinders of the nozzle needles. In particular, they were aimed at verifying the proper working of the overall system and have been performed by sending suitable signals to the control system. For instance, the complete closure of the main ball valve and some disturbances on the reference speed signal has been simulated.

Two different sets of tests have been carried out only on one of the two units, with the ball valve of the second unit completely closed.

The first set has regarded the correct functioning of the revamped control system of the needle actuators. These tests have been performed in standstill conditions with the main valve closed (no water load) and without electrical load. Considering the control block diagram of the needle position reported in Figure 6, the tests have been conducted by applying square and triangular wave reference signals G_0 to the position controller of the actuators. Experimental data acquired during these tests have been used to tune the parameters and the time constants of the models of the position controller, servovalve and actuators.

Two different anomalies affect the needles: the incomplete closure and the backlash. The incomplete closure is described in Figure 10 where the measured positions of all the needles are reported. In this case the same full stroke square wave reference command signal is applied to each controller of the needle actuators.

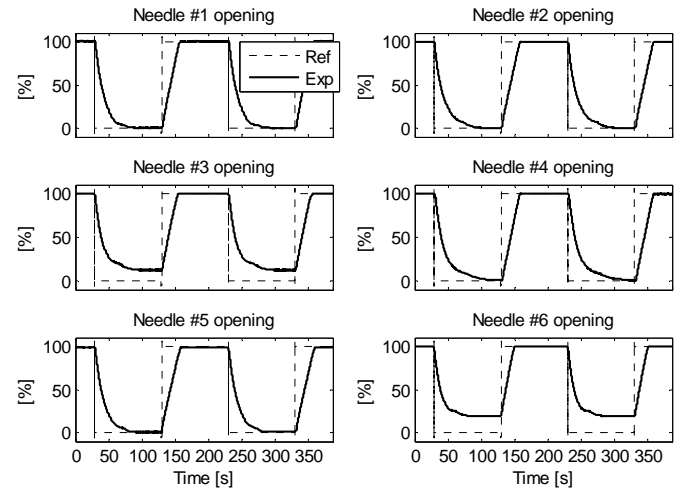


Figure 10. Position response of nozzle needles with square wave reference command signal: incomplete closure of needles #3 and #6.

It is possible to observe an incomplete closure of needles #3 and #6 whereas other needles share the same behaviour with a delay of about 50 s to reach the given full step input. The

different response between opening and closure phases is due to different maximum values of the cylinder oil flows. The incomplete closure of the needle affects only low loads operating condition.

The second and most important anomaly that affects some needle is the backlash between the hydraulic actuator and the needle itself and between the needle and its position transducer. Backlash is observable during the direction changes of the needle movement. For instance in Figure 11 the response of the needle #2 for a small triangular wave reference command signal is reported. It is possible to observe a delay of about 10 s between the measured response and the reference signal when the direction changes. Other needles, namely #4, showed the same behaviour.

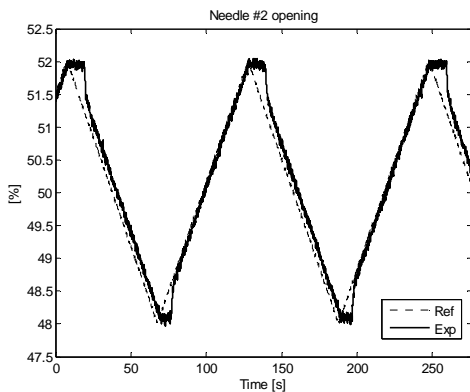


Figure 11. Position response of nozzle needle #2 with small triangular wave reference command signal: backlash effect during the direction change.

The anomalies of the needle movements are modelled and simulated. In Figure 12 and Figure 13 the simulated needle positions are reported for square and triangular wave reference signal respectively.

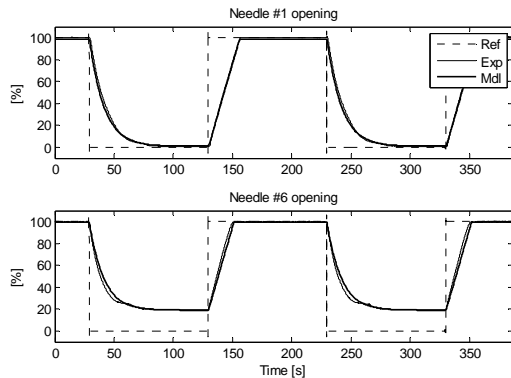


Figure 12. Reference, experimental and simulated response of needles #1 and #6 with square wave reference command signal.

The second set of tests has been carried out on the overall system, in order to test several operating conditions: the starting procedure from standstill to rated speed, the rated load

condition and other safety procedures.

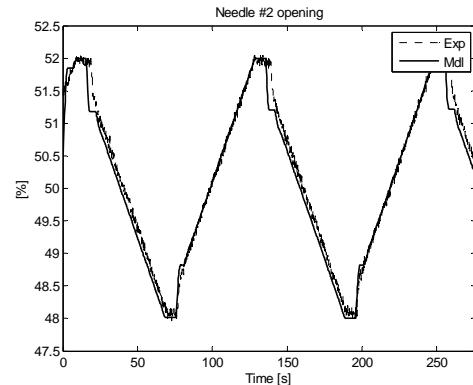


Figure 13. Experimental and simulated response of needles #2 with small triangular wave reference command signal.

In particular at the operating condition with a nominal load of 50 MW, an oscillation of the active power of about 8% appears, as shown in Figure 14. In the same figure the needle positions and the water pressure in the penstock at gate are also reported. The peaks of the electric power appear in correspondence of the discontinuities of some needles affected by backlash (e.g. needle #4). The same discontinuities are also associated to the peaks of the water pressure in the penstock.

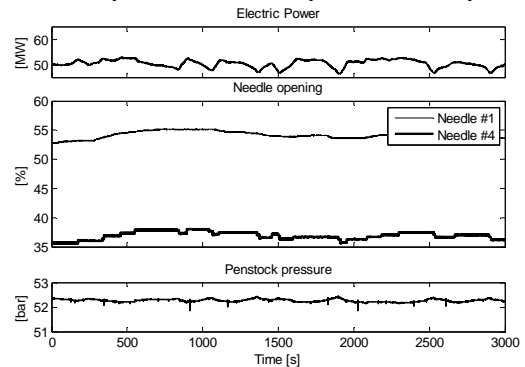


Figure 14. Electric power, needle openings and penstock pressure at 50 MW rated load.

The model of the overall system is used in order to investigate the causes of the electrical power oscillations. In particular, the simulations are performed at operating condition of 50 MW for the case without (Figure 15) and with (Figure 16) the needle backlash identified in the previous set of tests. As said before a constant electric torque is considered in the model. In Figure 15 the turbine speed remains almost constant, whereas the needle openings are the same for all the nozzles. The water pressure in the penstock shows only the long period oscillation due to the surge tank oscillations. In Figure 16 the effect of the backlash is evident on the discontinuous movement of the needles. These quick movements create water hammer phenomena in the penstock and oscillations of the turbine rotational speed. Considering the

constant electric torque used in the model, the oscillations of the turbine speed represent the electrical power oscillations.

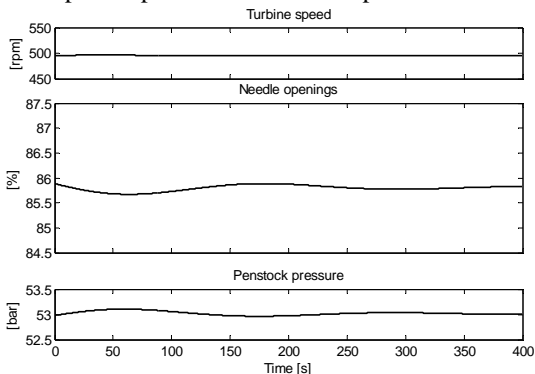


Figure 15. Simulations without needle backlash.

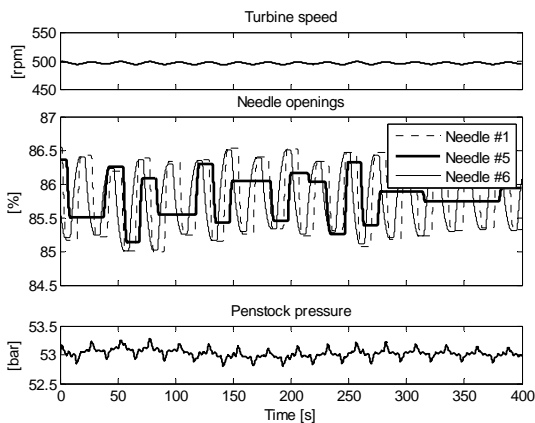


Figure 16. Simulation with needle backlash.

The oscillations of the electric power have been reduced by the plant conductor, by implementing a controller loop on the electric power. In Figure 17, the same quantities of Figure 14 are reported for an electrical load of 60 MW with the power control loop. In particular it is possible to observe a reduction of the oscillations on the active electric power and a long period oscillation of the water pressure in the penstock (about 250 s) owing to the water oscillations between the reservoir and the surge tank.

CONCLUSION

A detailed model of the overall plant of a Pelton turbine hydroelectric unit has been designed and successfully tested as described in the paper.

The model is developed with the transfer function approach and includes the servovalve and the hydraulic cylinder control loops, the effect of the travelling waves between the reservoir and the surge tank as well as the water hammer phenomenon.

It was tuned and verified by means of experimental data acquired during some inspection tests performed after a revamping of the distributor control unit and used as reference response in order to validate the required test of restoring

procedure of the same plant. The simulations have allowed the anomalous oscillations of the electric power at rated load to be mainly ascribed to the nozzle needle backlash.

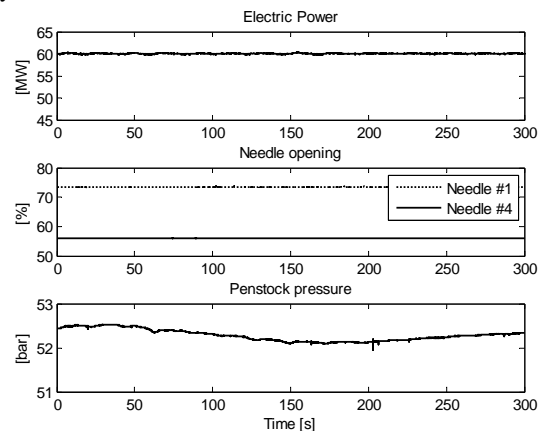


Figure 17. Electric power, needle openings and penstock pressure 60 MW load with power loop.

REFERENCES

1. Byerly R.T., Aanstad O., Berry D.H., Dunlop R.D., Ewart D.N., Fox B.M., Johnson L.H., Tschappat D.W., Dynamic models for steam and hydro turbines in power system studies, *IEEE Transactions on Power Apparatus and Systems*, Vol.PAS-92, No.6, (1973), pp.1904-1915.
2. Oldenburger R., Donelson Jr. J., Dynamic Response of a Hydroelectric Plant, *Transaction of the American Institute of Electrical Engineers*, Vol.81, No.3 (1962), pp.403-418.
3. Working Group on Prime Mover, Hydraulic turbine and turbine control models for system dynamic studies, *IEEE Transactions on Power System*, Vol.7, No.1 (1992), pp.167-179.
4. Pennacchi P., Chatterton S., Ricci R., Vania A., Modeling of the Dynamic Response of a Francis Turbine, *The 8th IFToMM International Conference on Rotor Dynamics*, Seoul, South Korea (2010), pp.1062-1068.
5. Borsetto M., Giuseppetti G., Martinetti S., Ribacchi R., Silvestri T., Design and construction of the Timpagrande powerhouse, *Rock Mechanics and Rock Engineering*, Vol.16, No.2, (1983), pp.85-115.
6. De Jaeger E., Janssens N., Malfliet B., Van De Meulebroeke F., Hydro Turbine model for system dynamic studies, *IEEE Transactions on Power Systems*, Vol.9, No.4, (1994), pp.1709-1715.
7. Kundur P., *Power system stability and control*, (1994), EPRI Editors.
8. Hannett L.N., Feltes J.W., Fardanesh B., Field tests to validate hydro turbine-governor model structure and parameters, *IEEE Transactions on Power System*, Vol.9, No.4, (1994), pp.1744-1751.
9. Okou F.A., Akhrif O., Dessaint L., A robust nonlinear multivariable controller for multimachine power systems, *Proceedings of the 2003 American Control Conference*, Vol.3, (2003), pp.2294-2299.
10. Catanese A., Barglaza M., Hora C., Numerical simulation of a free jet in Pelton turbine, *The 6th International Conference on Hydraulic Machinery and Hydrodynamics*, Timisoara, Romania, (2004), pp.79-84.